Lattice Defects in Sub-Micrometer Spin-Crossover Crystals Studied by Electron Diffraction

Hilaire Mba, Matthieu Picher, Nathalie Daro, Mathieu Marchivie, Philippe Guionneau, Guillaume Chastanet, Florian Banhart

Lattice Defects in Sub-Micrometer Spin-Crossover Crystals Studied by Electron Diffraction

Hilaire Mba[1], Matthieu Picher[1], Nathalie Daro[2], Mathieu Marchivie[2], Philippe Guionneau[2], Guillaume Chastanet[2], Florian Banhart[1]*

[1] Institut de Physique et Chimie des Matériaux, UMR 7504, Université de Strasbourg, CNRS, 67034 Strasbourg, France

[2] Université de Bordeaux, CNRS, Bordeaux INP, ICMCB, UMR 5026, 33600 Pessac, France

* florian.banhart@ipcms.unistra.fr

Abstract

Spin-crossover particles of $[Fe(Htrz)_2trz](BF_4)$ with sizes of some hundred nanometers are studied by *in-situ* electron microscopy. Despite their high radiation sensitivity, it was possible to analyze the particles in imaging and diffraction so that a detailed analysis of crystallographic defects in individual particles became possible. The presence of one or several tilt boundaries, where the tilt axis is the direction of the polymer chains, is detected in each particle. An *in-situ* exposure of the particles to temperature variations or short laser pulses to induce the spin crossover shows that the defect structure only changes after a high number of transformations between the low-spin and high-spin phases. The observations are explained by the anisotropy of the atomic architecture within the crystals that facilitates defects between weakly linked crystallographic planes.

Spin-crossover (SCO) materials, based on coordination complexes of metal ions either stacked through weak intermolecular interactions or linked into coordination polymer networks, have the property to switch between two phases with, in many cases, high differences of the volumes of the crystallographic unit-cells. The switching between the two phases, each corresponding to a defined spin state of the central metal ion, is achieved by heating or cooling, by exposure to light pulses, by pressure variations or by an external magnetic field.[1-6] In general, at low temperatures, the molecules are in the low-spin (LS) state while at a temperature above the transition point, they are in the high-spin (HS) state. When the central metal is iron(II), the volume of the coordination sphere is 25 % smaller in the LS state due to smaller metal-ligand bond lengths compared to the HS state. This ultimately affects the unit-cell and even macroscopic crystal volumes. To date, the reported unit-cell volume modifications at the LS to HS transition are in the range from -2% to +12 %.[6] The expansion or contraction of the crystal under changing external conditions (temperature, light, pressure) is in most cases reversible and anisotropic so that the expansion or contraction depends on the crystallographic direction. It is for example common that some unit-cell parameters strongly decrease while others strongly increase at the HS to LS spin transition and vice-versa.[5-7] SCO

crystals are therefore highly interesting candidates for photoswichable materials that change their morphology and global volume under laser pulses.

The crystallographic information about SCO materials has so far been obtained by X-ray diffraction, leading to a multiscale description of the switching phenomenon from the coordination sphere variation to the macroscopic mosaicity and crystal breathing.[3, 5, 6, 8-10] However, studying crystallographic properties in microscopic SCO particles at the single-particle level is still challenging. By contrast, diffraction and imaging by transmission electron microscopy (TEM) techniques allow studies at the microscopic scale with higher spatial resolution. The first TEM studies by ultrafast transmission electron microscopy (UTEM) have already revealed time-resolved information about the expansion dynamics of individual SCO particles under laser pulses.[11-14]

Structural defects in spin-crossover materials have an influence on the switching properties, e.g., on the overall lattice expansion during the spin transition or the width of the thermal hysteresis.[15-17] It has already been observed in X-ray diffraction that the crystallinity and the lattice parameters of $[Fe(Htrz)_2trz](BF_4)$ SCO particles in each spin state are affected by several heating-cooling cycles where the transformation between the LS and HS phase occurs.[15-17] It has been suggested that crystal defects might be responsible for the changes of the properties, but an identification of the exact nature of the defects by X-ray techniques hasn't been possible. It is therefore important to know about the presence and type of crystal defects in as-synthesized SCO particles and whether microstructural changes occur during heating or repeated phase transformations. This can be achieved by electron diffraction on single SCO particles, which is the goal of the present study.[11]

The lack of detailed electron microscopy studies of SCO materials is most likely due to their rapid degradation under electron irradiation. The difficulty of TEM studies of SCO materials is the tradeoff between the minimum electron dose to provide sufficient signal for imaging or diffraction and the maximum tolerable dose before the material degrades. This was undertaken in the present study on particles of the $[Fe(Htrz)_2trz](BF_4)$ 1D-coordination polymer that shows a thermally-induced spin transition with a thermal hysteresis between approximately 330 and 370 K. This compound has already been widely studied because of the memory effect that is highly reproducible,[18] either in nanoparticles or in microcrystalline powders[9, 19] and has been implemented in electronic devices.[20, 21] Here, the influence of repeated phase transformations between the LS and the HS state on the defect structure is studied *in-situ* by changing the specimen temperature and by subjecting the SCO particles to nanosecond laser pulses.

In this study, particles of $[Fe(Htrz)_2trz](BF_4)$ were synthesized in several batches by mixing 1.2 M of $Fe(BF_4)_2.6H_2O$ salt to three equivalents of 1*H*-1,2,4-triazole (Htrz), both dissolved in a 60%:40% water:ethanol mixture.[18, 22] The two solutions were mixed with magnetic stirring and let reacting during 15 min at 80°C. Then, the resulting mixture was cooled down to room temperature during 1h45, still with magnetic stirring. Finally, the precipitate was separated by centrifugation (8,000 rcf – 4 min), then washed with water

and twice with the same water – ethanol mixture. The resulting SCO particles were dispersed in ethanol and deposited on amorphous carbon films that were held by copper grids for electron microscopy studies. Scanning electron microscopy images of the particles are shown in the supporting information (Figs. SI 1-3). The particles are crystalline nanorods from different synthesis cycles with an orthorhombic lattice (space group *pnma*, a = 17.3474(16)Å, b = 7.3247(6) Å, c = 9.1907(9) Å in the low-spin phase at 300 K).[23] The sizes of SCO particles are between 600 nm and 1 µm in the b-axis direction and approximately 150 – 250 nm in the a- or c-axis direction of the lattice. As seen from the SEM images, the morphologies of the particles are quite different. The maximum expansion occurs in the b-direction and therefore along the long axis of the SCO particles.[13, 24]

Imaging and diffraction were carried out in two TEMs (Jeol 2100), one of them equipped with a laser system for ultrafast operation in a pump-probe mode.[13, 25] For the present study, a continuous electron beam was used. A heating stage allowed temperature changes and so to switch the particles between the low- and high-spin state under close-to-equilibrium conditions. The temperature range 290 – 400 K was studied, which reaches beyond the hysteresis of the LS-HS transition temperature (330 – 370 K) but remains below the amorphization temperature of approximately 590 K.[17] The expansion or contraction of the lattice during phase changes was determined in electron diffraction patterns. Alternatively, the samples were subjected to nanosecond laser pulses (7 ns duration, 532 nm wavelength) for *in-situ* observation of structural changes after a rapid phase transformation.[13]

Imaging in bright field and dark field was possible; however, lattice imaging in high resolution turned out to be impossible because the crystals are destroyed by electron irradiation before the necessary dose for lattice imaging is acquired. The maximum tolerable electron dose was determined by observing the amorphization and by measuring the expansion under temperature changes (see Sect. 3 in the supporting information). Electron irradiation did not lead to any observable changes of the size or lattice parameters of the particles so that changes of the spin state by electron irradiation can be excluded. Since we have also studied the SCO under nanosecond laser pulses without additional heating of the sample,[13, 14] the observed changes of the lattice parameter are not due to thermal expansion, which is small in this material in comparison to the expansion during the phase transition.[24] The measurable expansion only originates from the spin conversion.

Several as-synthesized SCO particles were first studied by imaging and electron diffraction at room temperature. Figure 1 shows a bright field and a dark field image of an SCO particle with the corresponding electron diffraction pattern. Due to the low electron dose, a certain noise level in the images and diffraction patterns could not be avoided. The b-direction (010) is slightly off the long axis of the particles (2-3°). Diffraction patterns of as-synthesized particles always show diffraction spots corresponding to two or more crystallographic orientations in the direction perpendicular to the b-axis of the particle. This indicates that the SCO particles are bicrystals or polycrystals where the domains are separated by tilt boundaries. The tilt axis is always the b-direction of the crystals. The diffraction patterns are therefore composed of spots from two or more crystals sharing a common b-axis within the particles. Selected-area

diffraction patterns taken at different positions along the long axis of the particles show no considerable changes, confirming that the normal on the boundary plane is always perpendicular to the b-direction and that there are no crystallographic changes in the b-direction. Due to the rod-like shape of the particles, they are always lying flat on the carbon grid so that the b-axis is in the grid plane and therefore perpendicular to the viewing direction. However, the deposition on the grid did not result in a preferential orientation in the a- or c-direction so that the viewing direction perpendicular to b is random and differs from particle to particle.

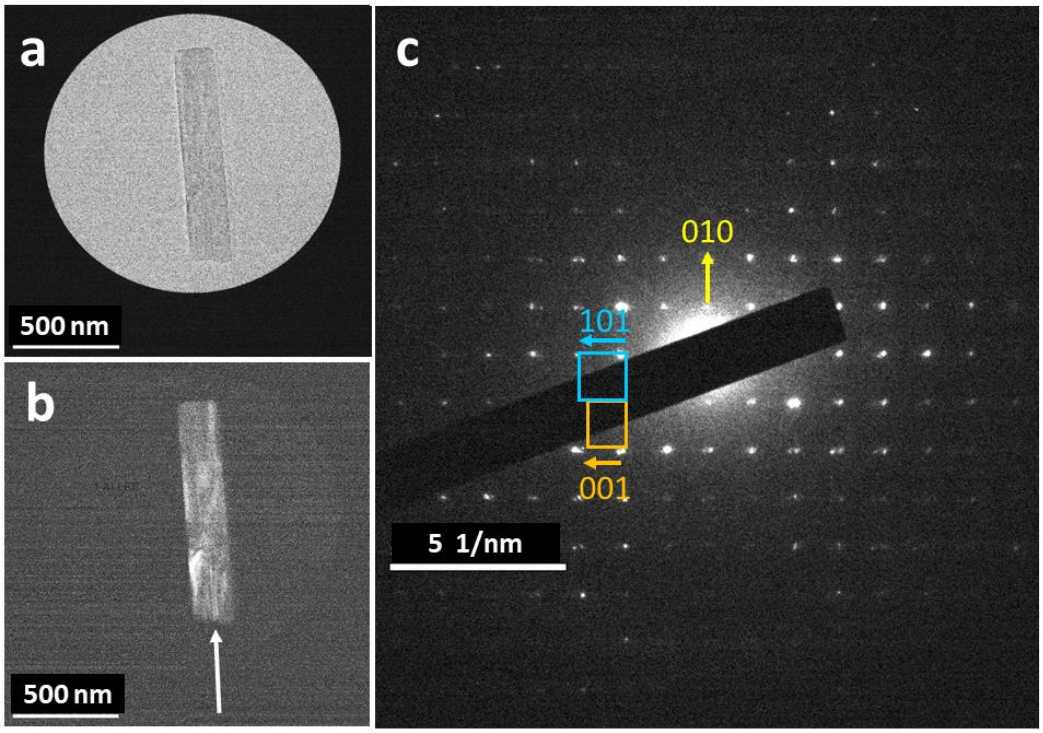

Figure 1: Bright field (a) and dark field (b) images of an SCO particle of $[Fe(Htrz)_2trz](BF_4)$ and the corresponding diffraction pattern (c). A linear contour along the b-direction is marked by an arrow. The doubling of spots in the diffraction pattern indicates the presence of two crystals with a relative tilt around the b-axis. The indexing of the reflections from the two components is shown in blue and orange color. The common b-axis is the (010)-direction (arrowed in yellow).

The images in Figs. 1a and 1b show several contours which are more prominent in dark field. The irregular contours move when the specimen is tilted, showing that they are bend contours and not related to defects. By measuring the position of bend contours in the b-direction as a function of the tilt angle of the specimen goniometer, an overall bending angle of some crystals along the b-axis of the order 3 – 4° can be estimated. However, some contours in dark field change their contrast but remain stationary when the diffraction conditions change. This indicates the presence of lattice defects. In dark field images, one or several linear contours

along the b-direction (long axis of the particle) are often found (arrowed in Fig. 1b). The SCO particle in Fig. 1 is close to a low-indexed zone axis for both components as seen from the symmetric diffraction pattern. The normally forbidden reflections (001) and (010) appear here due to dynamic diffraction effects. Most of the sufficiently intense diffraction spots are doubled, which is typical for the presence of a twin boundary or several twin boundaries on parallel planes. By measuring the spacings normal to the b-direction (010), the (101) and the (001) reflections can be identified (arrows in Fig. 1c). This would be roughly in accordance with a twin on the (-101) plane which contains the b-axis but is inclined relative to the image plane (see the discussion below and Fig. 5).

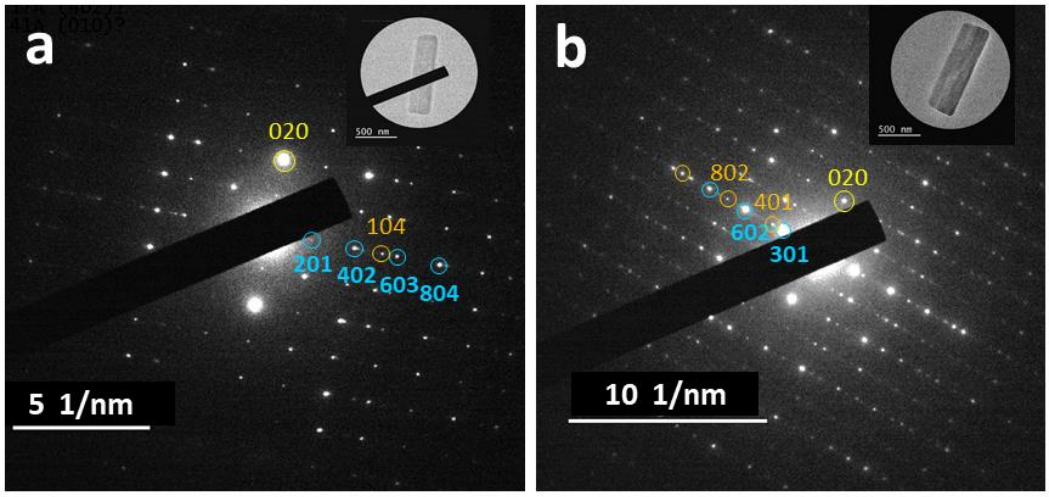

Figure 2: Electron diffraction patterns from two different SCO crystals of $[Fe(Htrz)_2trz](BF_4)$ (bright field images shown in the insets). (a): The (201)- and the (104)-series are visible, indicating a large-angle tilt boundary. (b): In this particle, the (301)- and (401)-spots are excited, in accordance with a low-angle tilt boundary.

Diffraction patterns from two other SCO particles are shown in Figure 2. In Fig. 2a, the (201)-reflection series of one component appears together with (104)-reflections of the other component. The angle between the (201)- and (104)-direction in the perfect lattice is 50° which should correspond to the tilt angle at the interface. In fig. 2b, the (301)- and the (401)-reflections appear together. The angle between these directions is only 2.5° and thus far from what would be expected for a {101}-twin, so a low-angle tilt boundary has to be assumed. Some further diffraction spots could not be attributed to the (301)- and the (401)-reflection series and arise from other domains. It is therefore a polycrystal with a common b-axis. Diffraction patterns from other SCO particles always show a tilt axis along (010) but different combinations of diffraction spots so that tilt boundaries with different angles prevail in different particles.

The as-synthesized particles were subjected to heating from room temperature to 400 K where the particles are in the HS phase. Cooling from 400 K to room temperature transforms the particles back to the LS phase. These heating-cooling cycles were repeated several times

to observe a possible influence of single or multiple phase transformations on the defect structure as it has already been indicated in X-ray studies.[23] A previous study by TEM imaging has already shown the expansion of similar SCO particles during the LS → HS transformation.[13, 14]

Figure 3 shows the anisotropic expansion of the lattice by imaging and electron diffraction (in reciprocal space, the expansion appears as contraction of the pattern). During the transformation, the lattice parameter in the b-direction ((020)-reflection) increases by 5.7 % (error ± 0.3 %) which is roughly in accordance with the expansion of 6.3 % as measured previously in $[Fe(Htrz)_2trz](BF_4)$ particles by X-ray diffraction.[23] In the (201)-direction, an expansion of 3.0 % appears, also roughly in accordance with the expected expansion of 1.2 % in the a- and 3.9% in the c-direction obtained by previous X-ray diffraction experiments. In the images (insets in figs. 3), the length of the particle along b increases by 5.8 % whereas an expansion of approximately 2 % is measured perpendicular to the long axis.

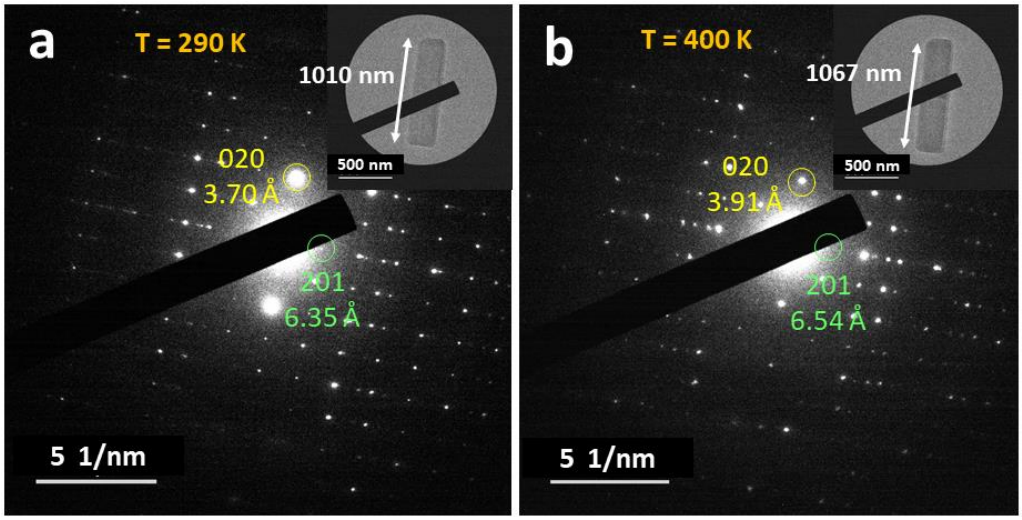

Figure 3: Diffraction patterns and images (insets) of a $[Fe(Htrz)_2trz](BF_4)$ crystal showing the lattice expansion (diffraction) and the size expansion (imaging) in the transformation from the low-spin (290 K) to the high-spin (400 K) phases of the same SCO particle. The maximum lattice expansion occurs in the b-direction.

The crystal in Fig. 3 (another crystal than shown in Figs. 1 and 2) has a tilt boundary like the crystals shown in Figure 2. The diffraction patterns at room temperature and at 400 K do not show considerable changes under heating so that the phase transformation between low- and high-spin and the size change of the lattice don't lead to restructuring or annealing effects within the particle. Successive cooling or repeated heating-cooling cycles (up to 10 cycles were carried out) don't show changes either. Furthermore, the duration of the high-temperature state doesn't seem to play a role. In diffraction patterns of the particle shown in Fig. 1, a vanishing of the double reflections upon repeated heating and cooling was observed;

however, it is not clearly confirmed that an annealing effect has occurred (shown in Sect. 2 of the supporting information)

Figure 4 shows the evolution of diffraction patterns when pristine (not previously heated) SCO particles at room temperature were irradiated with a sequence of laser pulses. In previous experiments by ultrafast TEM,[13, 14] it was shown that the LS → HS transformation occurs within some tens of nanoseconds whereas the transformation HS → LS occurs within the cooling time at the microsecond scale (depending on the power of the laser pulses and on the thermal conductivity of the substrate). Since the present experimental conditions are similar (laser power on the sample, wavelength and duration of laser pulses), we can assume that the transformation between the spin states happened after each laser pulse. As it can be seen in Fig. 4 the diffraction patterns of an SCO crystal with a tilt boundary don't show noticeable changes in the defect structure after one laser pulse (1 mJ/cm^2). However, after a long series of laser pulses (e.g. 1200 as in Fig. 4c), more diffraction spots along the direction perpendicular to the b-direction appear. This indicates the formation of new domains with a common b-axis when many phase transformations occur. Furthermore, a certain improvement of the crystallinity of the particle after many phase transformations is possible and has already been indicated in earlier X-ray studies, but only when the crystals were heated above 480 K.[8, 10] Here, a much higher number of transitions (Fig. 4c) is observed that happen under laser pulses, i.e., not under close-to-equilibrium conditions such as in slow temperature changes.

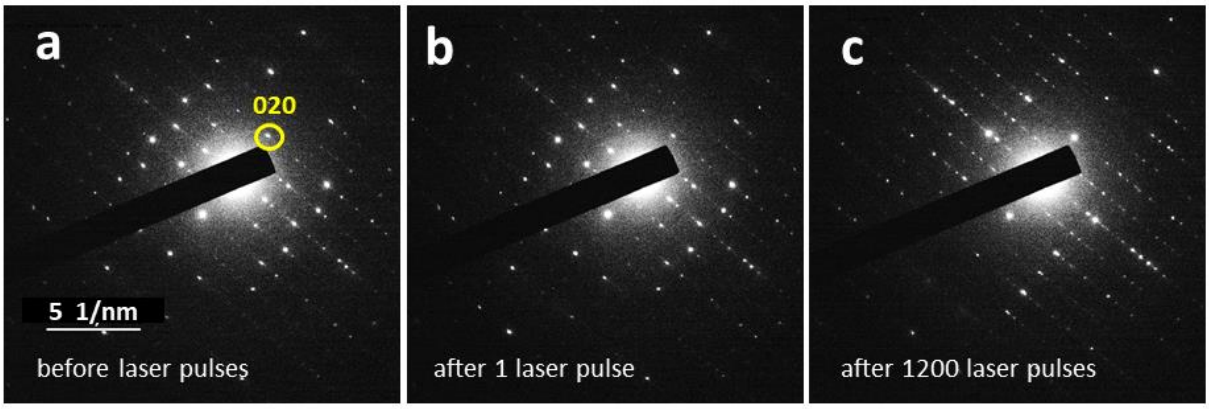

Figure 4: Diffraction patterns of an SCO crystal of $[Fe(Htrz)_2trz](BF_4)$ before (a), after one (b) and after 1200 (c) laser pulses (532 nm, 7 ns, 1 mJ/cm^2).

In the studied SCO compound, a possible rotation of the chains or the arrangement of the BF_4^- anions has already been seen by X-ray diffraction,[23] but isn't easily detectable by electron diffraction due to the high radiation sensitivity of the crystals and lower angular resolution of electron diffraction. As we have seen, different particles have boundaries with different tilt angles. This is also visible in the SEM images (Figs. SI 1-3) where most particles appear to be a composite of different domains.

The formation of the bi- or polycrystalline structure must already have occurred during the growth of the SCO crystals.[22] During the nucleation, the crystals grow along the b-axis which

is the direction of the polymer chains and the direction of the covalent bonds within the crystal structure. The growth of a particle appears to occur in two or more domains with a common b-axis but different orientations in a and c. If we assume growth in another direction, single or repeated formation of tilt boundaries must have happened during and not before growth. Since the crystals grow in solution during the synthesis of the $[Fe(Htrz)_2trz](BF_4)$ particles and the whole process is carried out under stirring, the turbulent liquid environment might be responsible for shear stress during growth and the formation of tilt boundaries. This points to the importance of finding appropriate growth conditions of SCO crystals in general. The weak chemical bonds normal to the polymer chains softens the crystal and facilitates deformation or the formation of planar defects on planes containing the "strong" direction (here along b).

Twins in orthorhombic crystals within the *Pnma* space group generally appear on the most densely packed {101}-planes. In the $[Fe(Htrz)_2trz](BF_4)$ SCO crystals, the quasi-infinite $[Fe(Htrz)_2trz]$-based chains along the b-direction are connected by hydrogen bonds in the a-b-plane, weaker by several orders of magnitude compared to covalent bonds, or indirectly through interactions with the anions.[23] The {101}-twin plane is therefore a plane of easy glide where the interface energy is low and shear could change the twin structure. Although the majority of the tilt boundaries observed here do not precisely correspond to a {101}-twin, a possible structure of a twin on a {101}-plane of $[Fe(Htrz)_2trz](BF_4)$ is shown in the model in Figure 5.

Orthorhombic crystals can be derived from a hexagonal lattice where the c-axis corresponds to the orthorhombic b-axis with a ratio a/c of $3^{1/2}$ = 1.73 for perfect hexagonal system. The ratio a/c for the present crystal (a/c = 1.88) is close to this value, and the crystal can be described as a pseudo-hexagonal system. A possible twin law in a hexagonal system is given by a rotation around the a- or b-axis, in accordance with the (-101)-direction observed here in the orthorhombic system. For a twin axis perfectly lying along the (-101) direction, an angle of 56° between the (100)-directions of the two domains would be expected. However, in this case, due to the orthorhombic distortion, the (001)-direction of domain 1 and the (101)-direction of domain 2 aren't perfectly aligned and a difference of 6° remains. So, to explain the observations in Fig. 1, an angle of 62° between the two domains prevails, and the twin plane slightly deviates from the expected {101} twin plane of a hexagonal system as shown in Figure 5. The deviation of the orthorhombic lattice from the hexagonal symmetry could thus explain the difference.

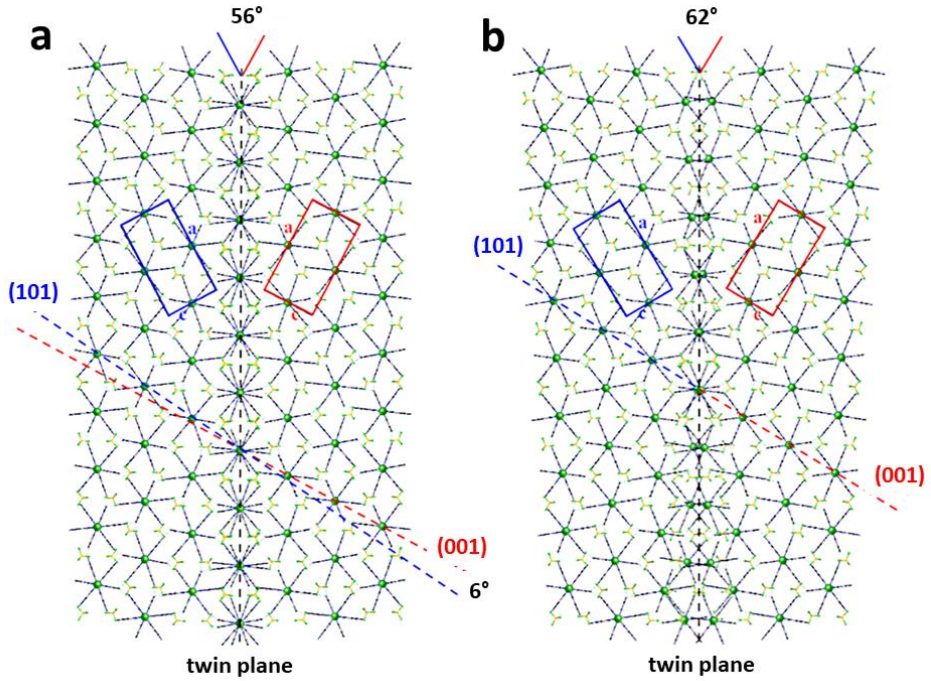

Figure 5: Model of a twin boundary on a {101}-plane of a $[Fe(Htrz)_2trz](BF_4)$ crystal. The crystal is viewed along the b-direction. The unit cells with the a- and c-axes of the two half-crystal components are depicted in blue and red. (a) A model of a twin exactly in the expected {101}-plane where the angle between both domain is 56° and (b) a model showing a twin where the twin plane slightly deviates from the expected {101}-plane leading to an angle of 62° between both domains so that both the (001) and the (101)-reflections appear together in the diffraction patterns.

A periodic lattice of twins (as, e.g., the 9R-structure in fcc-crystals) can't be assumed here due to the lack of clearly identifiable superlattice reflections. Other types of tilt boundaries with arbitrary tilt angles, as observed in this study, should also be possible. Due to the hydrogen bonds, the overall density of the $[Fe(Htrz)_2trz](BF_4)$ crystals is low (circa 1.8 kg m^{-3}) compared to inorganic compounds, and the stacking fault energy should be small, in particular on the {101}-plane. Other models such as the already observed mosaic structure of SCO crystals,[10] where the crystal domains are tilted by small angles (< 2°) relative to each other, can be excluded. A broadening of reflections in diffraction is not observed. Diffraction patterns from more than 20 crystals were taken, and each crystal showed these types of defects. Several of the observed defect structures could not be explained by a simple twin on a {101}-plane, and two or three macroscopic domains prevail. Hence, the twin structure exists but doesn't seem to be a particularly favorable configuration. Growth of two or more components under different tilt angles appears in most cases. A common type of tilt boundary (i.e., a typical tilt angle) could not be attributed. Since the {101}-interface should always be preferred, this observation isn't fully understood yet but should be related to the weak bonding between the polymer chains.

As we have shown, most of the observed tilt boundaries don't change their configuration under slow heating or under a few laser pulses. The transformation of the two half-crystal components at a tilt boundary into a single crystal would need considerable restructuring. This would require either high temperature, where the mobility of the atoms is sufficiently high (not expected at 400 K), or considerable shear stress along the interface and perpendicular to the b-direction. The previously observed changes of the properties of SCO crystals under heating and cooling and fatigue effects[15] are not observed here.

The increase of domains after many laser-induced phase transformations could be due to shear within the domains. The different expansions of the a- and c-lattices (1.2 % vs. 3.9 %) under the phase transformation LS – HS leads to a distortion of the lattice in the a-b-plane. Since the hydrogen bonds in the plane are weak and rather high temperatures prevail for a short duration during the laser pulse, a plastic shear deformation could happen so that the number of domains increases with time during the stroboscopic laser irradiation. The formation of small domains close to the surface of the particles appears more likely due to the easier glide under shear.

In conclusion, the first detailed imaging and diffraction study of individual spin-crossover nanoparticles by electron microscopy techniques shows that $[Fe(Htrz)_2trz](BF_4)$ particles don't grow as perfect single-crystals. Two or more domains with a tilt around the crystallographic b-axis appear so that there are different orientations of the a- and c-axes within one particle. However, the particles always have a common b-axis, which is an important fact because this is the direction of the covalent $[Fe(Htrz)_2trz]$ chains within the crystal and correspond to the maximum lattice expansion of the crystals during the spin transition. The expansion in any direction normal to the b-axis cannot be simply given by the known expansion in a and c but depends on the type of the defects. The angle and the position of the tilt boundaries have to be known to calculate the in-plane expansion. So, for the application of spin-crossover crystals as nanoswitches in which the size of the crystals is critical, the defect structure is playing an important role. The spin transition normally doesn't have a considerable influence on the tilt boundary. However, many fast switching cycles may lead to the formation of new domains due to repeated shear deformation of the lattice. The systematically observed formation of multiple domains with different crystal orientations in $[Fe(Htrz)_2trz](BF_4)$ particles synthetized by the literature protocols shows the importance of developing new synthesis routes to grow perfect SCO single crystals with higher perfection.

Acknowledgements

Funding by the Agence Nationale de la Recherche (contract ANR-22-CE09-0033-01) and the CNRS-CEA "METSA" French network (FR CNRS 3507) is gratefully acknowledged. The authors wish to thank T. Ferté and the SEM platform for supplying the SEM images.

References

(1) Kahn, O. Molecular magnetism, VCH Publishers, New York, NY **1993**.

(2) Gütlich, P.; Goodwin, H. A. (Eds.) Spin crossover in transition metal compounds I–III, Topics in Current Chemistry, **2004**, *233–235*.

(3) Halcrow, M. A. *Spin-crossover materials properties and applications*, Wiley, Chichester, UK **2013**.

(4) Chastanet, G.; Lorenc; M.; Bertoni, R.; Desplanches, C. Light-induced spin crossover—solution and solid-state processes. *C. R. Chimie* **2018**, *21,* 1075-1094.

(5) Collet, E.; Guionneau, P. Structural analysis of spin-crossover materials: from molecules to materials. *C. R. Chimie* **2018**, *21*, 1133-1151.

(6) Guionneau, P.; Marchivie, M.; Chastanet, G. Multiscale approach of spin crossover materials: a concept mixing russian dolls and domino effects. *Chem. Europ. J.* **2021**, *27*, 1483-1486.

(7) Lakhloufi, S.; Lemée-Cailleau, M. H.; Chastanet, G.; Rosa, P.; Daro, N.; Guionneau, P. Structural movies of the gradual spin-crossover in a molecular complex at various physical scales. *Phys. Chem. Chem. Phys.* **2016**, *18*, 28307-28315.

(8) Guionneau, P.; Lakhloufi, S.; Lemée-Cailleau, M. H.; Chastanet, G.; Rosa, P.; Mauriac, C.; Létard, J. F. Mosaicity and structural fatigability of a gradual spin-crossover single crystal. *Chem. Phys. Lett.* **2012**, *542*, 52-55.

(9) Moulet, L.; Daro, N.; Etrillard, C.; Létard, J. F.; Grosjean, A.; Guionneau, P. Rational control of spin-crossover particle sizes: from nano-to micro-rods of [Fe $(Htrz)_2(trz)](BF_4)$. *Magnetochem.* **2016**, *2*, 10.

(10) Lakhloufi, S.; Tailleur, E.; Guo, W.; Le Gac, F.; Marchivie, M.; Lemée-Cailleau, M. H.; Chastanet, G.; Guionneau, P. Mosaicity of spin-crossover crystals. *Crystals* **2018**, *8*, 363.

(11) van der Veen, R. M.; Kwon, O. H.; Tissot, A.; Hauser, A.; Zewail, A. H. Single-nanoparticle phase transitions visualized by four-dimensional electron microscopy. *Nature Chem.* **2013**, *5*, 395-402.

(12) Park, S. T.; van der Veen, R. M. Modeling nonequilibrium dynamics of phase transitions at the nanoscale: application to spin-crossover. *Struct. Dyn.* **2017**, *4*, 044028.

(13) Hu, Y.; Picher, M.; Tran, N. M.; Palluel, M.; Stoleriu, L.; Daro, N.; Mornet, S.; Enachescu, C.; Freysz, E.; Banhart, F.; Chastanet, G. Photo-thermal switching of individual plasmonically activated spin crossover nanoparticle imaged by ultrafast transmission electron microscopy. *Adv. Mat.* **2021**, *33*, 2105586.

(14) Hu, Y.; Picher, M.; Palluel, M.; Daro, N.; Freysz, E.; Stoleriu, L.; Enachescu, C.; Chastanet, G.; Banhart, F. Laser-driven transient phase oscillations in individual spin crossover particles. *Small* **2023**, 2303701.

(15) Grosjean, A.; Daro, N.; Pechev, S.; Moulet, L.; Etrillard, C.; Chastanet, G.; Guionneau, P. The spin-crossover phenomenon at the coherent-domains scale in 1D polymeric powders: evidence for structural fatigability. *Eur. J. Inorg. Chem.* **2016,** *13-14*, 1961-1966.

(16) Boukheddaden, K.; Traiche, R.; Oubouchou, H.; Linares, J. Multistep relaxations in a spin-crossover lattice with defect: a spatiotemporal study of the domain propagation. *Magnetochem.* **2016**, *2*, 17.

(17) Grosjean, A.; Daro, N.; Pechev, S.; Etrillard, C.; Chastanet, G.; Guionneau, P. Crystallinity and microstructural versatility in the spin-crossover polymeric material $[Fe(Htrz)_2(trz)](BF_4)$. *Eur. J. Inorg. Chem.* **2018***, 3-4*, 429-434.

(18) Kroeber, J.; Audiere, J. P.; Claude, R.; Codjovi, E.; Kahn, O.; Haasnoot, J. G.; Grolière, F.; Jay, C.; Bousseksou, A.; Linarès, J.; Varret, F.; Gonthier-Vassal, A. Spin transitions and thermal hysteresis in the molecular-based materials $[Fe\ (Htrz)_2(trz)](BF_4)$ and $[FeHtrz)_3](BF_4)\ 2H_2O$ (Htrz= 1, 2, 4-4H-triazole; trz= 1, 2, 4-triazolato). *Chem. Mater.* **1994**, *6*, 1404-1412.

(19) Coronado, E.; Galán-Mascarós, J. R.; Monrabal-Capilla, M.; García-Martínez, J.; Pardo-Ibáñez, P. Bistable spin-crossover nanoparticles showing magnetic thermal hysteresis near room temperature. *Adv. Mater.* **2007**, *19*, 1359-1361.

(20) Molnar, G.; Rat, S.; Salmon, L.; Nicolazzi, W.; Bousseksou, A. Spin crossover nanomaterials: from fundamental concepts to devices. *Adv. Mater*. **2018**, *30*, 17003862.

(21) Gavara-Edo, M.; Cordoba, R.; Valverde-Munoz, F. J.; Herrero-Martin, J.; Real, J. A.; Coronado, E.; Electrical sensing of the thermal and light-induced spin transition in robust contactless spin crossover/graphene hybrid devices. *Adv. Mater*. **2022**, *34*, 2202551.

(22) Palluel, M.; El Khoury, L.; Daro, N.; Buffière, S.; Josse, M.; Marchivie, M.; Chastanet, G. Rational direct synthesis of $[Fe\ (Htrz)_2(trz)](BF_4)$ polymorphs: temperature and concentration effects. *Inorg. Chem. Frontiers* **2021**, *8*, 3697-3706.

(23) Grosjean, A.; Négrier, P.; Bordet, P.; Etrillard, C.; Mondieig, D.; Pechev, S.; Pechev, E.; Lebraud, J.-F.; Létard, P.; Guionneau, P. Crystal structures and spin crossover in the polymeric material $[Fe\ (htrz)_2(trz)](BF_4)$ including coherent-domain size reduction effects. *Eur, J. Inorg. Chem.* **2013**, *5-6*, 796-802.

(24) Palluel, M.; Tran, N. M.; Daro, N.; Buffière, S.; Mornet, S.; Freysz, E.; Chastanet, G. The interplay between surface plasmon resonance and switching properties in gold@spin crossover nanocomposites. *Adv. Funct. Mater.* **2020**, *30*, 2000447.

(25) Picher, M.; Bücker, K.; LaGrange, T.; Banhart, F. Imaging and electron energy-loss spectroscopy using single nanosecond electron pulses. *Ultramicroscopy* **2018**, *188*, 41-47.